Virtual Shear Checkshot from a densely sampled DAS walkaway VSP in a desert environment

Ali Aldawood[1]*, Amnah Samarin[1], Ali Shaiban[1] and Andrey Bakulin.

Summary

Distributed Acoustic Sensing (DAS) provides a cost-effective method for recording borehole seismic surveys. DAS can measure only a single component of strain or strain rate, making it unsuitable for 3-component processing necessary to separate mode-converted waves, unlike conventional 3C geophone Vertical Seismic Profile (VSP) data. However, in moderately deviated wells equipped with optical fibres, DAS can accurately capture high-fidelity mode-converted events even at significant source offsets from the well. Recently, DAS VSP data was acquired in a desert environment, revealing mode-converted energy across the deviated part of the well from shots spanning an offset range between 1.5 km to 2.7 km. The virtual source method, also known as seismic interferometry, was applied to this mode-converted energy to create virtual shear sources igniting mainly shear-wave energy inside the borehole. The method was basically utilised to transform the walkaway DAS VSP data into single-well profiling or virtual checkshot, enabling precise measurements of shear-wave seismic velocities. The obtained velocity profiles from the virtual downhole shear sources closely match the velocities acquired from the dipole sonic log and geophone VSP data in an adjacent well. These results underscore the effectiveness of seismic interferometry in obtaining accurate shear-wave velocity profiles, even from single-component DAS measurements.

Introduction

Distributed Acoustic Sensing (DAS) has proven to be a relatively inexpensive tool to record seismic signals (Zhan, 2020). It has been widely used in borehole seismic acquisition since it provides a dense array of recording points along the fibre at a relatively low cost (Mateeva et al., 2014). DAS vertical-seismic-profiling (VSP) are increasingly acquired and demonstrated as a replacement for conventional geophone surveys (Yu et al., 2020), particularly for 4D seismic and reservoir monitoring (Mateeva et al., 2013, 2014; Isaenkov et al., 2022). DAS uses fibre-optic cables as a sensing array to record seismic data instead of the three-component geophones used in VSP acquisition surveys (Yu et al., 2018) by measuring the axial strain or strain rate along the fibre (Bakku, 2015). Cables are often installed inside wellbores, resulting in a large downhole seismic array for VSP imaging and monitoring (Yu et al., 2019). Downhole wireline geophones typically have a fixed spacing of around 15 m, and the array's length is limited to a few hundred metres, which are often moved multiple times to cover the desired depth range (Titov et al., 2022). Enhancing the density of VSP data poses a significant challenge with traditional geophone receivers, necessitating innovative acquisition methods such as DAS. The DAS receiver acts as a natural array, providing an average over the gauge length while enabling dense receiver sampling (Bakulin et al., 2020). Optical fibres enable complete well coverage in a single sweep, offering high receiver densities at a more affordable cost (Yu et al., 2019). Fibre-optic cables are now commonly deployed in wellbores for real-time pressure and temperature monitoring during production (Fitzel et al., 2015). These pre-installed cables can capture borehole seismic data without wellbore intervention, with the assistance of a seismic vibrator and an interrogation box for recording optical signals. Different VSP acquisition geometries and cable conveyance methods, including on-tubing, behind the casing, and wireline, have been effectively utilised in successful DAS VSP field tests for subsurface imaging and monitoring (Hartog et al., 2014, Mateeva et al., 2014, Parker et al., 2014). Eliminating the need to move the tool string due to DAS covering the entire well enabled the acquisition of a multi-well 3D VSP survey (Mateeva et al., 2014). Aldawood et al. (2023) presented initial findings from their simultaneous dual-well DAS walkaway VSP acquisition. Their study showcased the potential of pre-installed DAS on production tubing, revealing high-resolution subsurface models and delivering high-quality imaging between two deep wells. This study shows an advanced analysis of this dataset focusing on harvesting valuable subsurface information using mode-converted waves.

In one well, we found clear mode-converted (PS) waves in the recorded data. We utilised the virtual source method (VSM) or seismic interferometry, leveraging these signals. This method enabled the creation of virtual shear sources in the downhole environment (Bakulin and Calvert, 2005, 2006; Schuster, 2009). The interferometric transformation enabled us to redatum

[1] Saudi Aramco

* Corresponding author, E-mail: ali.dawood.18@aramco.com

DOI: 10.3997/1365-2397.fb2024001

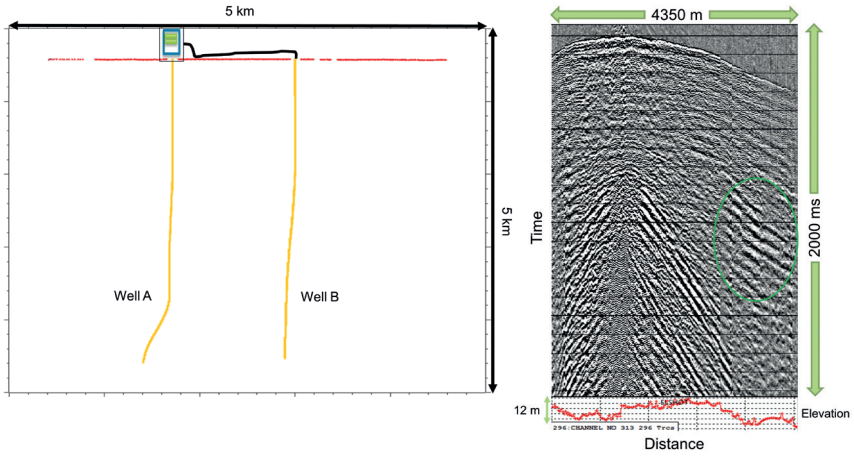

Figure 1 Dual-well acquisition set-up and data: (a) the acquisition geometry featuring the deviated well A and nearly vertical well B connected to the interrogator through a jumper cable (black); (b) a representative receiver gather at a depth of 2 km, highlighting distinct mode-converted arrivals indicated by green oval.

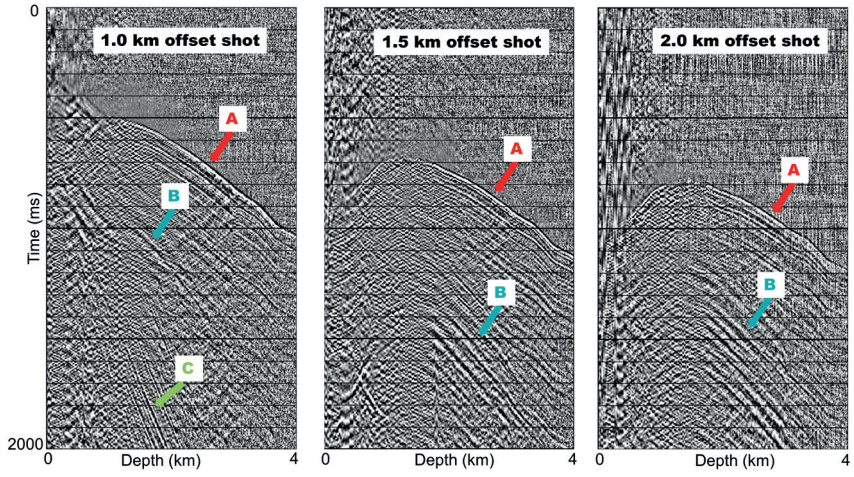

Figure 2 Three typical shot gathers from different offsets from the well showing the direct arrival event (A), the mode-converted PS arrivals (B), and the slow tube-waves (C).

surface shots to virtual sources inside the borehole using recorded data as natural wavefield extrapolation (Bakulin et al., 2007; Schuster, 2009). Thus, physically recorded data as walkaway VSP is transformed into a virtual single-well profiling (SWP) dataset. Bakulin et al. (2007) and Aldawood et al. (2019) showcased the reliability of S-wave velocity profiles derived from redatumed sources using 3C geophone walkaway VSP datasets. This study extends this method to single-component DAS walkaway VSP data. We aim to obtain an accurate shear-wave velocity profile similar to sonic log results, utilising the cost-effective DAS technology.

DAS walkaway VSP data

The survey utilised two pre-installed optical fibres in adjacent deep wells, spaced approximately 1.5 km apart, within a desert environment. In Figure 1a, the acquisition geometry is illustrated, with yellow dots representing receivers inside the boreholes (639 in well A and 630 in well B), and red dots indicating 292 surface shot locations spaced about 12.5 m apart. Both wells have a depth of approximately 4 km, and for this experiment, a gauge length (GL) of 24 m was set, with receiver spacing at 6.4 m. The GL refers to the length of the optical fibre over which the recorded signal is optically averaged (Dean et al., 2017). Both fibres are linked to the same interrogator, enabling simultaneous data recording from each shot point. In well B, the fibre is connected to the box through a jumper cable (black), as depicted in Figure 1a.

Figure 1b displays common-receiver gather from a depth of approximately 2 km at well A, highlighting evident mode-converted (PS) arrivals indicated by green oval. These PS arrivals are discernible within an offset range extending from around 1.5 km to 2.75 km towards well B. Shots within this range are employed in the interferometric redatuming process. Additionally, the elevation curve of the shots is depicted in Figure 1b, illustrating varying topography that contributes to significant statics in the first-arrival waveforms. Figure 2 displays three representative shot gathers captured at well A with offsets of 1 km, 2 km, and 2.5 km towards well B. Event A represents the P-wave initial arrival, while event B signifies the mode-converted arrival, and event C denotes the slow tube wave. Notably, event B exhibits a distinct slope and slower velocity in contrast to event A, the P-wave first arrival. This is evidence of capturing the mode-converted shear waves at these larger offsets from well A.

We applied a processing workflow to the DAS VSP dataset recorded at well A tailored to enhance downgoing mode-converted PS energy. These gathers are subsequently used for the interferometric transformation. Figure 3a shows the processing workflow for shear-wave profiling using the virtual source method. It starts with the first-break (FB) picking of the downgoing P-wave first arrivals followed by FB flattening and median filtering of the downgoing P-wave energy. The resultant wavefield consists of upgoing energy and downgoing mode-converted waves. Dip-median filtering is applied to amplify the upgoing P-wave reflections, crucial for imaging as demonstrated in Aldawood et al. (2023). Meanwhile,

the remaining wavefield, rich in downgoing mode-converted PS energy, is harnessed in the interferometric redatuming process. It's essential to highlight that the wavefield separation operations are confined to median and dip median filters due to the nature of the recorded DAS signals, which strictly represent single-component strain measurements along the optical fibre (Sayed and Stewart, 2020). Figure 3b shows the effect of the processing sequence on three representative shot DAS VSP gathers at varying offsets from the well. These processed DAS VSP shot gathers were inputted into the interferometric redatuming engine, resulting in the creation of the targeted shear-wave downhole virtual gathers.

Interferometric redatuming with virtual shear source

Seismic interferometric redatuming aims to convert the traditionally acquired walkaway VSP dataset into a virtual dataset with an altered acquisition set-up called single-well profiling (SWP). This transformed geometry (VSP → SWP transformation) situates both sources and receivers inside the borehole, achieved by moving surface sources to downhole receiver positions (Bakulin and Calvert, 2006; Schuster, 2009). The VSP-to-SWP interferometric redatuming is performed by applying the reciprocity equation of the correlation type (Wapenaar and Fokkema, 2006; Schuster, 2009) which in the frequency domain is written as follows:

$$\sum_{s=1}^{N} G\left(r_2|s\right)\, G\left(r_1|s\right)^{*} = G\left(r_2|r_1\right)^{virtual} \qquad (1)$$

where $G(r2|r1)$ represents a virtual SWP trace recorded at a deeper receiver station r_2 due to a virtual downhole shear source at a shallower receiver station r_1. $G(r_2|s)$ is the recorded DAS VSP seismic trace containing the extracted mode-converted PS arrivals recorded at r_2 due to a surface source at s. $G(r_1|s)^*$ is the complex conjugate of the recorded DAS VSP trace recorded at a receiver station r_1 due to a source at s. Note that the multiplication with the complex conjugate in the frequency domain is equivalent to the cross-correlation with the same trace in the time domain.

A schematic ray diagram in Figure 4a illustrates the geometrical interpretation of the cross-correlation between a mode-converted PS arrival recorded at r_2 due to a source at s and another mode-converted PS arrival recorded at r_2 due to a source at s. This operation results in a single-well profiling trace, representing a virtual shear-wave source ignited at a shallow receiver r_1 and recorded at a deeper receiver r_2. The travel time linked to the shared ray path is subtracted, and the arrival time of the virtual event corresponds to a direct shear energy propagating from r_1 to r_2. The virtual trace is obtained through a data-driven cross-correlation process between recorded traces, without relying on the subsurface velocity model. Importantly, redatuming the surface seismic eliminates the source-side statics (as shown in Figure 1b), providing a significant advantage (Schuster, 2009).

Bakulin et al. (2007) demonstrated that the use of a deviated well enhances the effectiveness of the Virtual Source Method

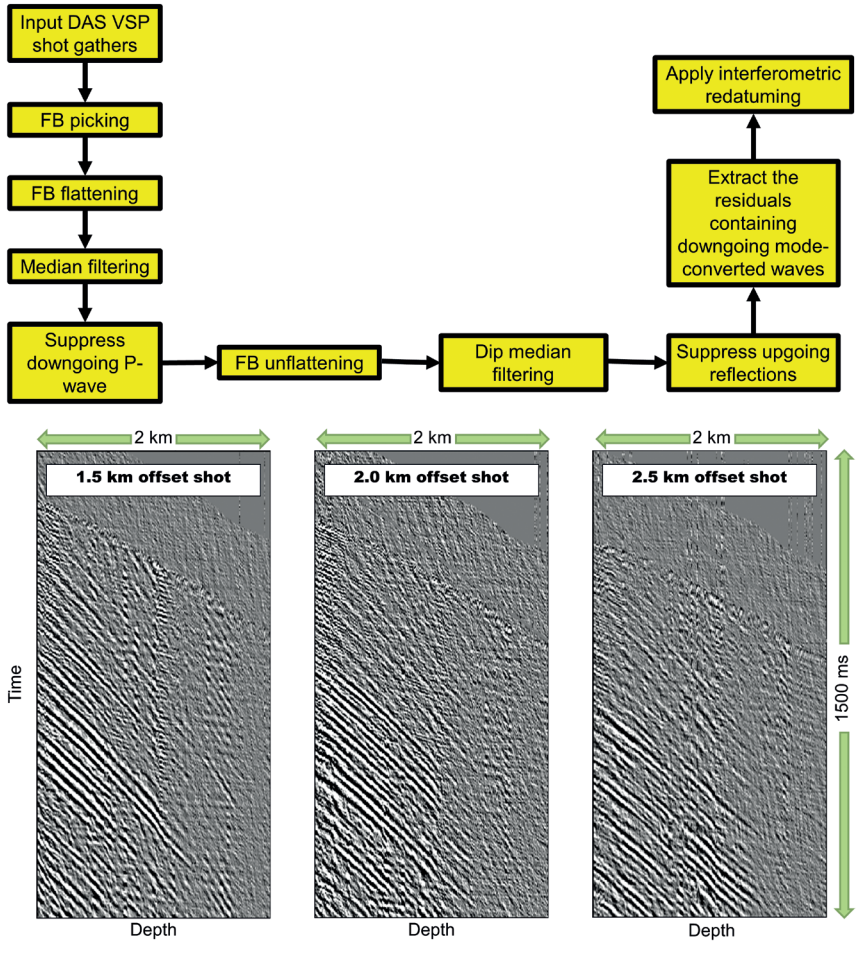

Figure 3 DAS data pre-processing and result: (a) The processing workflow used to extract downgoing mode-converted waves; and (b) three representative shot gathers at varying offsets showing enhanced PS arrivals after pre-processing.

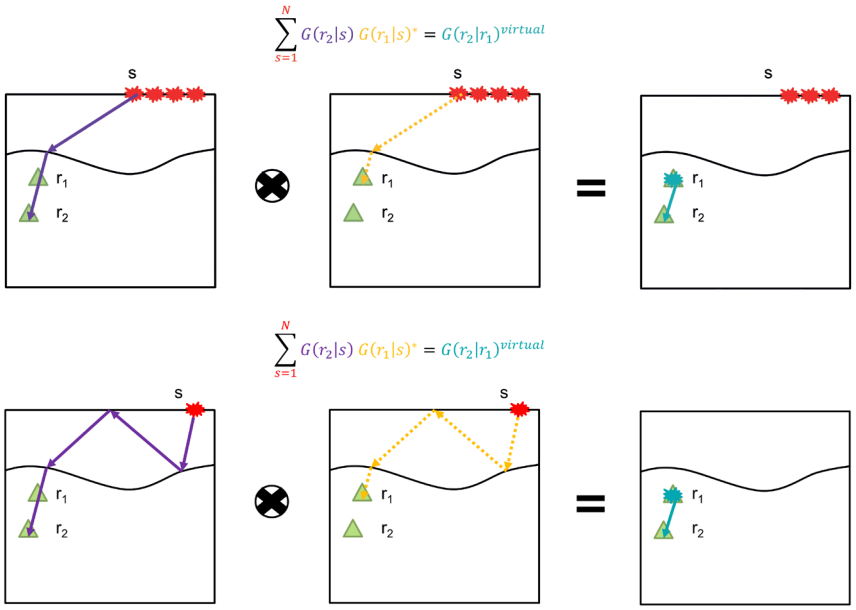

Figure 4 Interferometric redatuming illustrated: (a) a schematic Figure demonstrating cross-correlation redatuming of surface shots into a virtual downhole shot emitting shear-waves; and (b) a schematic Figure showing the advantage of including the recorded multiples in the interferometric transformation.

because it allows the downhole virtual source to effectively combine all mode-converted waves at non-vertical angles, as illustrated in Figure 4a. Consequently, stacking all shots within the offset range exhibiting mode-converted waves (1.5 km to 2.7 km offset in our study) results in precise shear-wave arrivals in the deviated well. These shots, as identified through stationary phase analysis, provide substantial physical contributions to the data (Korneev and Bakulin, 2006; Poliannikov and Willis, 2011). In well A, a comparable maximum deviation of approximately 26° from the vertical aligns with the field and synthetic examples presented by Bakulin et al. (2007). Their study utilised the horizontal component of the wavefield, primarily consisting of PS arrivals, for the interferometric transformation. In our DAS case, advanced processing of the single-component wavefield was necessary to separate the mode-converted arrivals. To enhance the reconstruction of virtual SWP shear-wave arrivals, we incorporated all mode-converted arrivals in the interferometric transformation. This strategic approach enables the constructive contribution of multiples of different orders to the desired downhole arrival, as depicted schematically in Figure 4b.

Results and discussion

A total of 233 downhole shear-source virtual gathers, ranging in depth from approximately 2000 m to nearly 3600 m in true vertical depth (TVD), were reconstructed using the interferometric transformation outlined in equation (1). This process redatumed and concentrated 140 surface shots, crucial for constructive interferometric stacking, at the downhole receiver positions illustrated in Figure 5a along the well trajectory. Figure 5b displays three illustrative virtual shear-wave shots corresponding to various virtual-source depths, ranging from shallow to deep within the reconstructed depth range. The picked arrivals on these virtual shots exhibit distinct event moveouts. In Figure 5b, four delineated zones highlight notable velocity changes, represented by varying slopes of the events. It's evident that there's a subtle overlap in the FB picks of the shear-wave direct arrival on the virtual shots across different zones. Zones 1 and 3 demonstrate slower shear-wave velocities, whereas Zones 2 and 4 display comparatively faster ones.

More than 16,000 shear-wave first-break (FB) picks were employed to reconstruct a partial profile spanning from a true vertical depth (TVD) of approximately 2000 m to 4000 m.

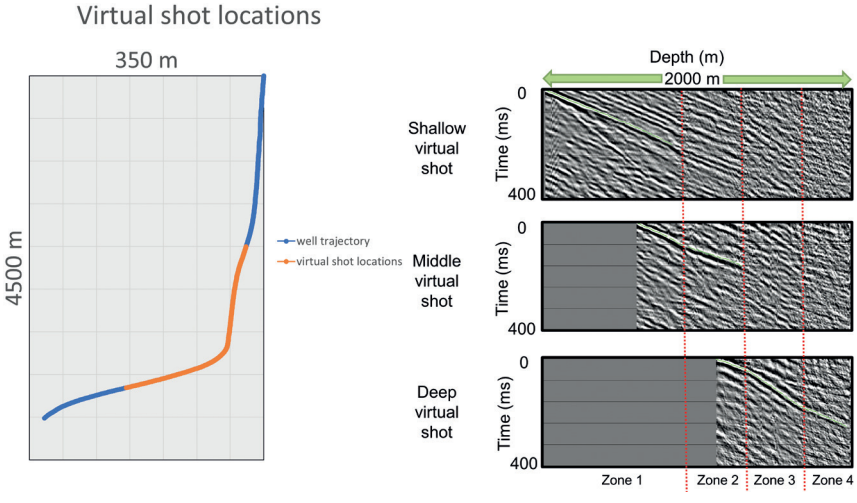

Figure 5 The virtual shear source reconstruction: (a) the virtual source locations with accurate reconstruction of the shear-source wavefield; and (b) three sample virtual shot gathers from shallow, intermediate, and deep locations within the reconstructed range. Distinct zones were delineated, each exhibiting unique slopes. The green dots highlight first-arrival picks of shear-wave energy.

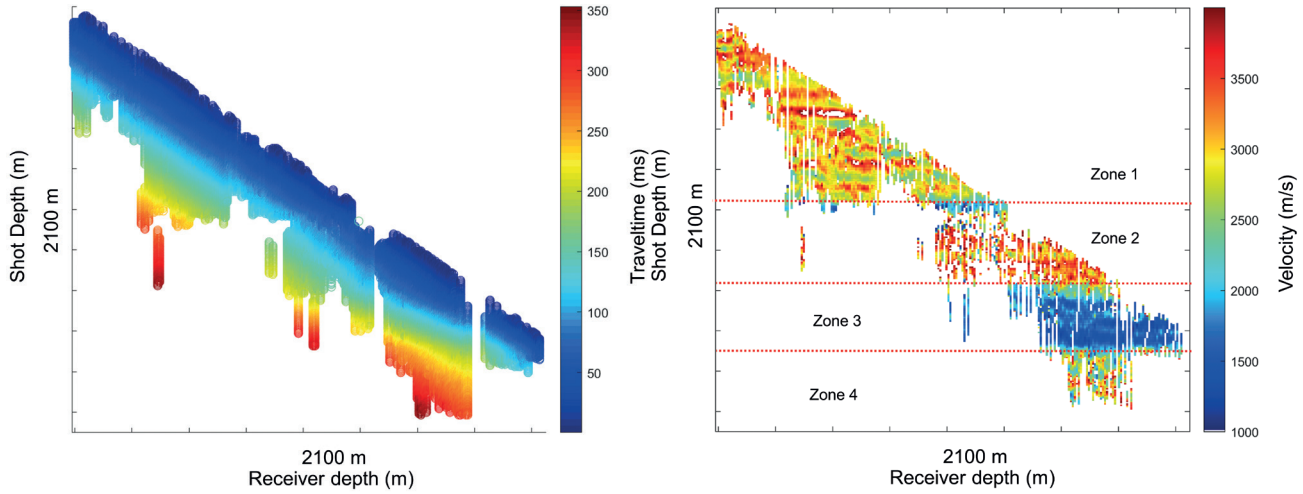

Figure 6 Shear-Wave Profiling: (a) More than 16,000 first-break picks were meticulously chosen for each virtual shot gather, covering a specific segment of the receiver depth range. All these picks contributed to constructing profiles in (b); (b) a total of 233 shear-wave velocity profiles across a depth range of approximately 2 km. Distinct boundaries outlining four different velocity zones are clearly discernible, as indicated by the red lines.

Figure 6a and 6b present all the picks after a 13-sample point linear-fit smoothing, and their corresponding 233 profiles, respectively. Notably, the four distinct zones are clearly delineated in Figure 6b.

We used all the reconstructed profiles to deduce the mean shear-wave velocity profile (in blue) with its standard deviation (in red) and presented the results in Figure 7. The black arrows mark the boundaries separating the different zones with lithology. The description of the cutting samples confirms these boundaries. The initial demarcation between Zone 1 and Zone 2 signifies the transition from clastic rocks featuring shale, siltstone, and sandstone interbeds to dolomitic lime mudstone. The subsequent boundary, distinguishing Zone 2 from Zone 3, indicates the presence of a distinct shale layer underlying the dolomitic lime mudstone. The third interface marks an unconformity between the shale in Zone 2 and a formation consisting of interbedded anhydrite, shale, and dolomitic lime mudstone. Therefore, the lithology change provides a strong validation of the virtually constructed shear-velocity profile.

To confirm the accuracy of the obtained shear-wave velocity profile, we superimposed the reconstructed profile in Figure 7 with a shear sonic-log profile from the nearby well B. The dashed black curve represents the shear sonic log, which aligns closely with the profile obtained using the virtual source method.

Previously, zero-offset VSP (ZVSP) dataset was collected in well B, and Alford rotation (Alford, 1986) was employed on the ZVSP datasets to extract both radial and transverse components. Shear-wave arrivals were identified to reconstruct shear-wave velocity profiles on the radial component, spanning the interface between Zone 3 and Zone 4, where a pure shale layer overlays a carbonate formation. Figure 8a displays the selected radial component geophone ZVSP gather, while Figure 8b showcases a single virtual DAS gather across the same depth range along the interface.

The shear-wave velocity profile obtained from the radial component geophone picks is illustrated in Figure 9 in yellow. It shows a remarkable agreement with the mean profile derived from the virtual gathers across the interface, indicated by the red arrow. The dashed black curve represents the shear-wave sonic from the neighbouring well, providing additional validation for the accuracy of the constructed profile using seismic interferometry. The discrepancy between the log and the seismic profiles, especially below the interface can be related to the fractures within this depth interval. It is a highly fractured zone that often shows strong shear-wave splitting effect; thus, it can yield different measurements for sonic and seismic depending on the azimuth of the tools and shot locations.

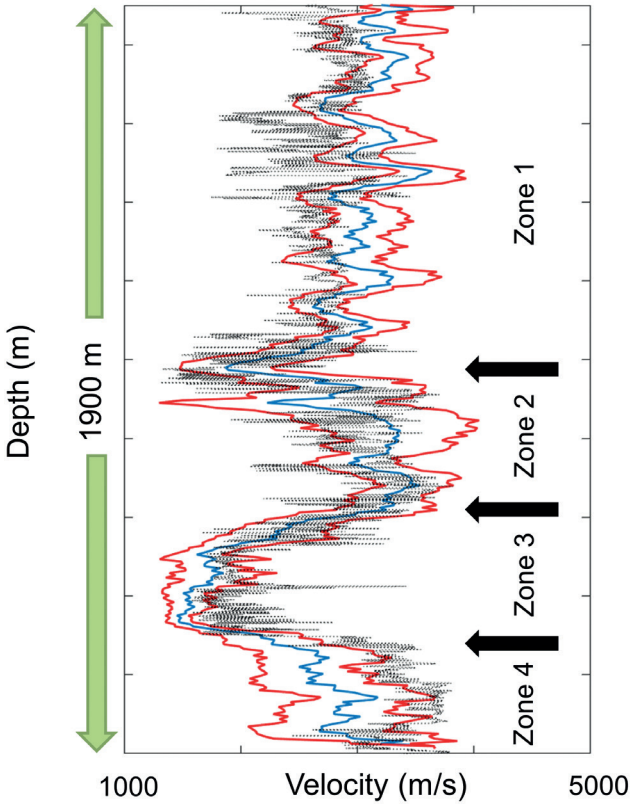

Figure 7 the average shear-wave profile depicted in blue, derived from all 233 profiles shown in Figure 6b. The corresponding standard deviation is represented in red. The black dashed curve represents the shear sonic log from the adjacent well B.

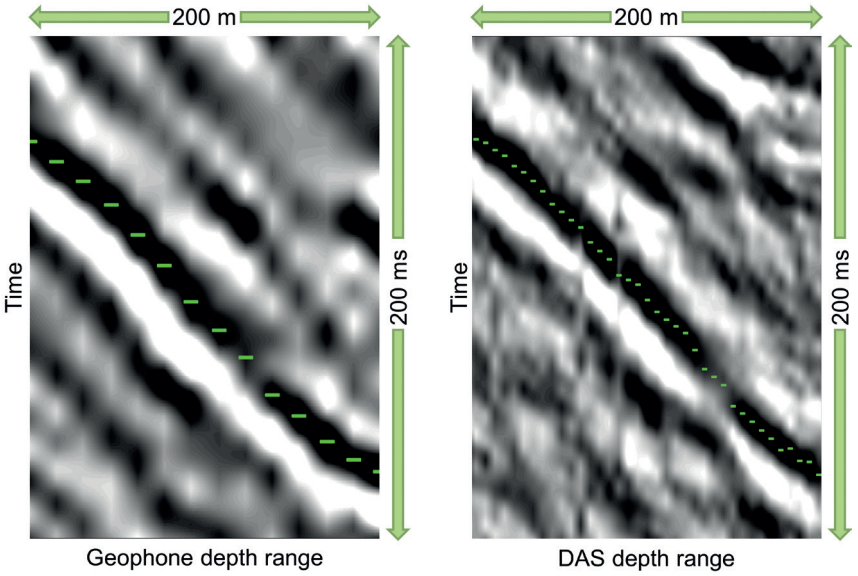

Figure 8 Shear-wave picking on: (a) the radial component of the ZVSP data spanning a depth range of 200 m across the boundary between Zone 3 and Zone 4; and (b) the virtual DAS downhole shear-source gather over the corresponding depth range. Note that the time in the radial component geophone data is the absolute time from the surface to downhole whereas the virtual DAS gathers shows the same time interval using the relative times after interferometric redatuming.

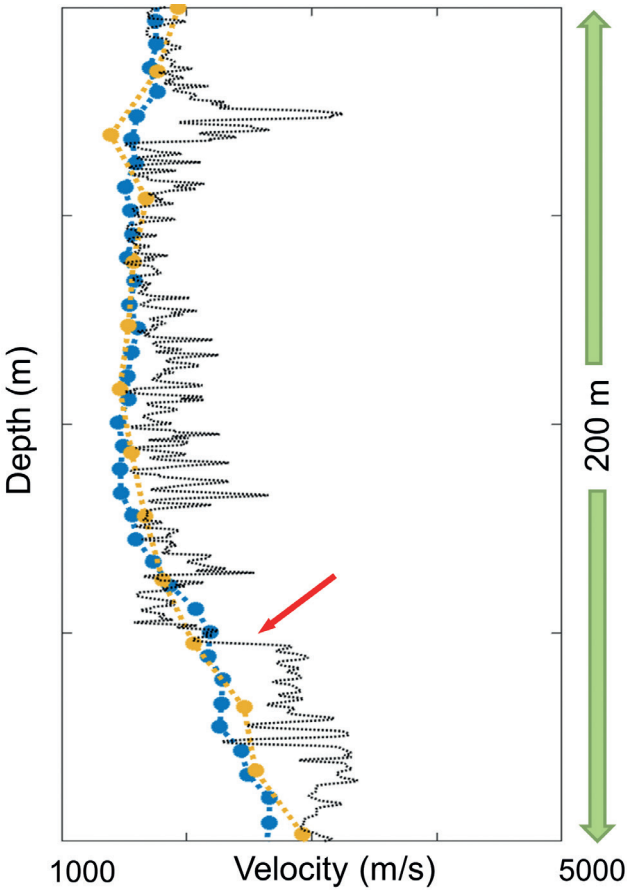

Figure 9 Comparison of shear-wave velocity estimates across the same interval in Figure 8. The yellow line represents data from the radial component of the ZVSP data (Figure 8a), while blue dots depict virtual shear checkshots from DAS data (Figure 8b). The shear log from the neighbouring well B is shown as a dashed black curve. Notice the strong agreement between geophone and DAS profiles, as well as alignment with the sonic log, indicating the accuracy and reliability of the obtained shear-wave velocity data.

Conclusions

In this study, we successfully applied the virtual source method to reconstruct downhole shear-wave sources using a recently acquired walkaway DAS VSP dataset in a desert environment. The recorded data exhibited reliable mode-converted waves from specific shots at offsets ranging from 1.5 to 2.7 km, particularly at deeper receiver stations within the deviated section of the well.

These selected shots, producing consistent stationary contributions, were utilised in a correlation-type interferometric redatuming operation. The resulting virtual downhole shot gathers, containing direct shear-wave energy, enabled the reconstruction of a robust shear-wave velocity profile from depths of approximately 2 to 4 km. The average velocity profile, derived from all the gathers, was calculated alongside the standard deviation, showcasing the reliability of the reconstruction.

Remarkably, the shear sonic log from a nearby well closely matched the reconstructed profile obtained through interferometry. This alignment revealed four distinct lithological zones, a finding corroborated by drill cutting samples.

To further validate the profile's robustness, we compared the reconstructed profile from picks on the radial component geophone with the mean profile derived from the DAS virtual shear gathers across a specific interface. The consistency between these profiles emphasised the reliability and accuracy of our methodology.

In summary, our study demonstrates the efficacy of the virtual source method in reconstructing shear-wave sources from DAS VSP data, offering valuable insights into subsurface structures and confirming the method's applicability for geological investigations in challenging desert environments.

References

Aldawood, A., Shaiban, A., Alfataierge, E. and Bakulin, A. [2023]. Acquiring and processing deep dual-well DAS walkaway VSP in an onshore desert environment. *The Leading Edge*, **42**(10), 676-682.

Aldawood, A., Silvestrov, I. and Bakulin, A. [2019]. Virtual Shear-Wave Source Delivers a Reliable S-Wave Velocity Model for VSP Imaging. 81st EAGE Conference and Exhibition 2019 *(Vol. 2019, No. 1, pp. 1-5)*, European Association of Geoscientists & Engineers.

Alford, R.M. [1986]. Shear data in the presence of azimuthal anisotropy. *SEG Technical Program Expanded Abstracts 1986*, Society of Exploration Geophysicists, pp. 476-479.

Bakku, S.K. [2015]. *Fracture characterization from seismic measurements in a borehole*. Doctoral dissertation, Massachusetts Institute of Technology.

Bakulin, A. and Calvert, R. [2005]. Virtual Shear Source: a new method for shear-wave seismic surveys. 75th Annual International Meeting, SEG, *Expanded Abstracts*, 2633-2636.

Bakulin, A. and Calvert, R. [2006]. The virtual source method: Theory and case study. *Geophysics*, **71**(4), pp.SI139-SI150.

Barrientos, C., Wielemaker, E., Plona, T.J., Haldorsen, J.B.U., Saldungaray, P. and Franco, L.A. [2006]. Emerging technology for quantifying minimal anisotropy. *First Break*, **24**(9).

Bakulin, A., Mateeva, A., Calvert, R., Jorgensen, P. and Lopez, J. [2007]. Virtual shear source makes shear waves with air guns. *Geophysics*, **72**(2), pp.A7-A11.

Bakulin, A., Silvestrov, I. and Pevzner, R. [2020]. Surface seismic with DAS: an emerging alternative to modern point-sensor acquisitions. *The Leading Edge*, **39**(11), 808-818

Dean, T., Cuny, T. and Hartog, A.H. [2017]. The effect of gauge length on axially incident P-waves measured using fibre optic distributed vibration sensing. *Geophysical Prospecting*, **65**(1), pp.184-193.

Fitzel, S., Sekar, B.K., Alvarez, D. and Gulewicz, D. [2015]. *Gas injection EOR optimization using fiber-optic logging with DTS and DAS for remedial work*. SPE/CSUR Unconventional Resources Conference. OnePetro.

Hartog, A., Frignet, B., Mackie, D. and Clark, M. [2014]. Vertical seismic optical profiling on wireline logging cable. *Geophysical Prospecting*, **62**(4), pp.693-701.

Isaenkov, R., Tertyshnikov, K., Yurikov, A., Shashkin, P. and Pevzner, R. [2022]. Effect of Source Mispositioning on the Repeatability of 4D Vertical Seismic Profiling Acquired with Distributed Acoustic Sensors. *Sensors*, **22**(24), p.9742.

Korneev, V. and Bakulin, A. [2006]. On the fundamentals of the virtual source method. *Geophysics*, **71**(3), A13-A17.

Mateeva, A., Lopez, J., Mestayer, J., Wills, P., Cox, B., Kiyashchenko, D., Yang, Z., Berlang, W., Detomo, R. and Grandi, S. [2013]. Distributed acoustic sensing for reservoir monitoring with VSP. *The Leading Edge*, **32**(10), pp.1278-1283.

Mateeva A. Lopez J. Potters H. Mestayer J. Cox B. Kiyashchenko D. Wills P. Grandi S. Hornman K., and Kuvshinov B. [2014]. Distributed acoustic sensing for reservoir monitoring with vertical seismic profiling, *Geophysical Prospecting*. **62**(4), 679-692, doi: https://doi.org/10.1111/1365-2478.12116.

Parker, T., Shatalin, S. and Farhadiroushan, M. [2014]. Distributed Acoustic Sensing – a new tool for seismic applications. *First Break*, **32**(2).

Poliannikov, O.V. and Willis, M.E. [2011]. Interferometric correlogram-space analysis. *Geophysics*, **76**(1), SA9-SA17.

Sayed, A., Ali, S. and Stewart, R.R. [2020]. Distributed acoustic sensing (DAS) to velocity transform and its benefits. *SEG Technical Program Expanded Abstracts 2020*, pp. 3788-3792.

Schuster, G. [2009]. *Seismic Interferometry*. Cambridge University Press.

Titov, A., Kazei, V., AlDawood, A., Alfataierge, E., Bakulin, A. and Osypov, K. [2022]. Quantification of DAS VSP quality: SNR vs. log-based metrics: *Sensors*, **22**(3), p.1027.

Wapenaar, K. and Fokkema, J. [2006]. Green's function representations for seismic interferometry. *Geophysics*, **71**(4), SI33-SI46.

Yu, G., Cai, Z., Chen, Y., Wang, X., Zhang, Q., Li, Y., Wang, Y., Liu, C., Zhao, B. and Greer, J. [2018]. Borehole seismic survey using multimode optical fibers in a hybrid wireline. *Measurement*, **125**, pp.694-703.

Yu, G., Chen, Y.Z., Wu, J., Li, Y.P., Li, F., Hu, G.M., Ran, Z.L. and Rao, Y.J. [2019]. 3D-VSP survey using a DAS system and downhole geophone array in Southwest China. 81st EAGE Conference and Exhibition 2019, (*Vol. 2019, No. 1, pp. 1-5*), European Association of Geoscientists & Engineers.

Yu, G., Xiong, J.L., Wu, J.J., Chen, Y.Z. and Zhao, Y.S. [2020]. Enhanced surface seismic data processing using simultaneous acquired DAS-VSP data: *First Break*, **38**(6), pp.29-36.

Zhan, Z. [2020]. Distributed acoustic sensing turns fiber-optic cables into sensitive seismic antennas. *Seismological Research Letters*, **91**(1), pp.1-15.